Radiative Heating Profiles in Simple Cirrus Cloud Systems

ANDREW DETWILER

Institute of Atmospheric Sciences, South Dakota School of Mines and Technology, Rapid City, South Dakota

V. RAMASWAMY

Atmospheric and Oceanic Sciences Program, Princeton University, Princeton, New Jersey

(Manuscript received 19 September 1989, in final form 26 March 1990)

ABSTRACT

Results from one-dimensional cirrus cloud model simulations in the absence of upward velocities are used to show that the growth/sublimation of the ice particles in the cloud, and the fact that they are falling, can be important factors in determining the net heating rate in the air through which these clouds settle. The vertical profiles of the heating rate inside the cloud are stretched as a result of the settling of the cloud. Results for clouds at various altitudes in both midlatitude and tropical atmospheres are compared.

1. Introduction

Cirrus clouds, that is, clouds composed almost exclusively of ice crystals, are present a large portion of the time in the upper troposphere over any particular location. The dynamics of the circulations responsible for the presence of cirrus in these regions, and the cloud microphysical properties, are such that individual cirrus cloud regions typically persist for many hours, although individual cells within these regions may have shorter lifetimes (Heymsfield 1975; Sassen et al. 1989). Cloud regions persisting for such periods of time will be affected strongly by radiative processes. Although the magnitude of radiative processes is not always locally as great as some of the other forcing important to cloud evolution, the fact that radiative processes act broadly and continuously over periods of a half-day or longer renders their integrated effects important during the evolution of a cirrus cloud region.

Among the many published studies of cirrus clouds there have been several investigations, both observational and computational, in which the radiative heating rates in cirrus clouds have been estimated and related to cloud microphysical and dynamical processes. Griffith et al. (1980) and Paltridge and Platt (1981) have used in situ microphysical and radiative flux measurements to investigate radiative heating rates. Ackerman et al. (1988) combined cloud top microphysical information with satellite radiances to deduce tropical anvil physical and radiative characteristics.

Hall and Pruppacher (1976), Welch et al. (1980), Wendling (1980), and Stephens (1983) explored theoretically the radiative properties of ice clouds and the influence of radiation on deposition/sublimation of ice particles. Starr and Cox (1985a,b) and Starr (1987) present results from a two-dimensional cloud model, including radiative interactions. Ramaswamy and Detwiler (1986) looked at interactions between radiative and microphysical processes in a one-dimensional layer cloud model.

Of particular relevance to the matters to be considered below are the vertical profiles of the various terms in the cloud thermal energy budget in Starr's model results. They are generally characterized by energy terms due to phase changes (deposition on, or sublimation from, ice particles) directly opposing radiative heating terms. That is, at cloud top, the radiative cooling is countered by latent heat release due to depositional growth of ice. At cloud base, where net radiative heating generally occurs, evaporative cooling of roughly equal magnitude also occurs. Thicker clouds had more pronounced relative peaks near base and top in both latent heating and radiative heating profiles.

Danielsen (1982a) used measurements from tropical anvils (Danielsen 1982b; Knollenberg et al. 1982) to advance the hypothesis that radiative heating from below and cooling at the top could destabilize tropical cirrus anvil clouds. He further conjectured that such destabilized anvils would rise above tropopause levels, with cloud top regions cooling adiabatically during ascent to temperatures lower than local tropopause air temperatures.

Corresponding author address: Dr. A. Detwiler, Institute of Atmospheric Sciences, South Dakota School of Mines and Technology, 501 E. St. Joseph Street, Rapid City, SD 57701-3995.

Ackerman et al. (1988) and Lilly (1988) further considered Danielsen's hypothesis concerning the destabilization of stratiform cirrus anvil clouds due to differential radiative heating at cloud base and cloud top. Lilly used radiative heating profiles from Ackerman et al. in a study of anvil outflow dynamics. In both studies, radiative heating rates were used as total heating rates, although in each discussion there was mention that this approximation introduced some uncertainty about the generality of the conclusions. The overall conclusion was that relatively thin, moderately dense anvils that are also not too wide may behave as Danielsen hypothesized. That is, due to differential radiative heating, they may become convective and rise, with their tops becoming colder than the surrounding air just above the local tropopause.

The qualitative role of radiation in cirrus cloud thermal energy budgets can be estimated using the results of the studies cited above. Radiative terms may clearly dominate in at least some circumstances. There is need for further refinement in delineating exactly which circumstances these are. To this end, further calculations have been carried out using a refined version of the one-dimensional settling cirrus cloud layer model of Ramaswamy and Detwiler (1986). The goal is to look at how a simple cloud layer's properties evolve with time. Particular attention will be paid to defining regimes in which latent heat exchange strongly counters radiative heating in layer clouds and those in which they do not. The influence of cloud settling on net heating within a specific altitude range will also be considered.

2. The computational experiment

The one-dimensional cirrus cloud model used here is described in detail in Ramaswamy and Detwiler (1986). It considers a cloud of bullet-shaped ice particles settling through a nonisothermal atmosphere. Particle geometry follows from relations given in Heymsfield (1972) for bullets. The cloud is divided into twenty 100 m thick layers with monodisperse particle size distributions and homogeneous temperature, pressure, and humidity within each layer. Cloud and air properties can vary from layer to layer. Detailed microphysical growth calculations treat the growth of ice particles from the vapor phase, including the role of radiation in the particle energy balance.

Particles are treated conceptually as randomly-oriented ice bullets. Optical constants for ice are taken from Warren (1984). Optical cross sections for absorption, scattering, and extinction at a given wavelength are computed using the Mie theory for spheres of equal surface area. Absorption by gases in the cloud is ignored.

A delta-Eddington approach (Wiscombe 1977) is used to calculate upward and downward radiative fluxes through the cloud in 56 solar bands (covering the visible and near infrared) and the infrared window (8–12 μm). Fluxes are computed at each of the 21 boundaries of the 20 layers. Incoming fluxes are specified at the upper and lower boundaries. Outgoing fluxes, and fluxes across internal boundaries, are found from the solution to the delta-Eddington system of coupled equations, given the specified incoming fluxes and the assumption of continuity in the intensity field at internal boundaries between each of the 20 layers.

Microphysical growth and particle settling is computed with a simple forward difference integration scheme using a 1-sec time step. The in-cloud radiative flux profiles are updated at 1 min intervals. Particle nucleation, aggregation, and breakup are not considered in the simple model. Particle motion relative to the air is computed, but motion of the air itself is not considered.

This model has been used to explore several relatively simple situations, including the evolution of aircraft contrails (Detwiler and Pratt 1984), midlatitude cirrostratus (Ramaswamy and Detwiler 1986), and (with enhancements to the microphysical parameterizations required by lower temperatures and also allowing for polydisperse particle size distributions within a layer) polar stratospheric clouds (Ramaswamy 1988).

For the simulations discussed below, the following enhancements were made to the model as presented in Ramaswamy and Detwiler (1986). Incident radiative fluxes are specified as a function of altitude and allowed to change as the cloud settles to lower altitudes, whereas previously the incident fluxes were considered constant through a simulation period. These flux profiles are computed for clear midlatitude and tropical standard atmospheres using the radiative transfer model of Ramaswamy and Kiehl (1985). Surface albedo is 0.1, and zenith angle is 60°. The profiles are shown in Fig. 1 and are assumed to be constant at a given altitude during a simulation. They do not reflect the possible influence of the cloud on the environment as it evolves and settles.

A second enhancement was to explicitly track the net heating of the air through which the ice particles settle. It must be remembered that cirrus clouds typically contain at least some particles with appreciable fallspeeds. If these particles predominate radiatively, then any absorbed radiation they convert to net thermal heating of nearby air will not be communicated to a fixed volume of air, but to a continuous stream of air as they fall. They cannot, in general, be treated as static sources/sinks of heat.

Twenty-minute simulations of cirrus cloud layers settling through the two different standard atmospheres were performed for three different positions within each atmosphere. The standard cloud properties are given in Table 1. Additional simulations were done while varying cloud microphysical characteristics, one at a time, relative to these standard conditions.

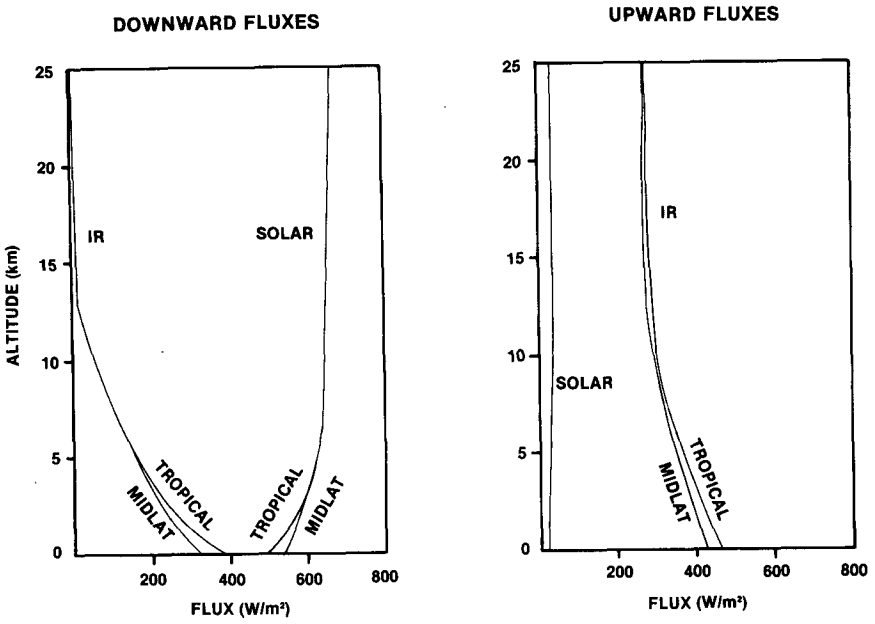

FIG. 1. Radiative flux profiles in the atmosphere in which cirrus layers were inserted.

The standard cloud characteristics were chosen to represent realistic cirrus cloud layer properties, and to be similar to the properties used in prior computational studies. The choices were somewhat arbitrary. They represent a relatively crude approximation to real cirrus clouds that are typically horizontally inhomogeneous and finite, where new particles are continually nucleating, and that typically contain very broad particle size spectra. The particle sizes used here are to be taken as representing a surface area mean size. Although Ackerman et al. (1988) chose to use a log normal number distribution peaked at 50 μm in their computations based on aircraft measurements in the tops of tropical anvils (corresponding to a surface area mean size of ~ 100 μm), one might infer a typical surface area mean size somewhat larger based on more comprehensive measurements in cirrus (Heymsfield and Platt 1984) and other anvils (Griffith et al. 1980; Bennetts and Ouldridge 1984; Heymsfield 1986; and Foot 1988).

TABLE 1. The initial physical properties of the cloud layers are shown above. The cloud top in the tropical atmosphere is at 14 km; in the midlatitude atmosphere it is at 12 km.

Standard cloud properties	
Thickness (m)	2 000
Particle size (μm)	150
Particle concentration (l)	150
Ice saturation ratio in cloud	1.01
Ice saturation ratio below cloud	.85
Visible optical thickness	.75
Ice water path $\frac{g}{m^2}$	84

Results of the simulations are intended to be used only to infer the sensitivity of total heating profiles to variations in microphysical and environmental conditions in a very simple situation, and not to generate precise predictions of cirrus cloud behavior in general.

3. Results

Results using the standard set of parameters listed in Table 1 are shown in Fig. 2. Figure 2 shows the ice water content profiles for a) midlatitude, and b) tropical cases initially and after 20 minutes. The tropical cloud falls further because it is falling through less dense air. Evaporation near cloud base is evident in both final cloud profiles, but strongest in the midlatitude case.

The model is so basic that simulations discussed herein will extend to only tens of minutes. Certainly, as time goes on, the behavior of a real cloud will be dominated by external factors not treated by the model, such as atmospheric dynamics; and also by internal factors, such as the polydispersity of particle sizes, nucleation of new particles, aggregation and/or breakup of old particles.

Earlier work with a version of this model (Detwiler and Pratt 1984) showed that time scales for the simulated dissipation of aircraft contrails simply settling into dry air could be as short as tens of minutes in a typical upper troposphere environment. Simulations with the current version, starting with properties as given in Table 1, suggest cloud lifetimes on the order of hours. The main differences are: 1) difference in initial cloud thickness, 100 m in the case of the contrails as compared to 2 km in the present case; and 2) higher subcloud saturation ratio in the current simulations, 0.85 compared to 0.50 in the contrail simulations.

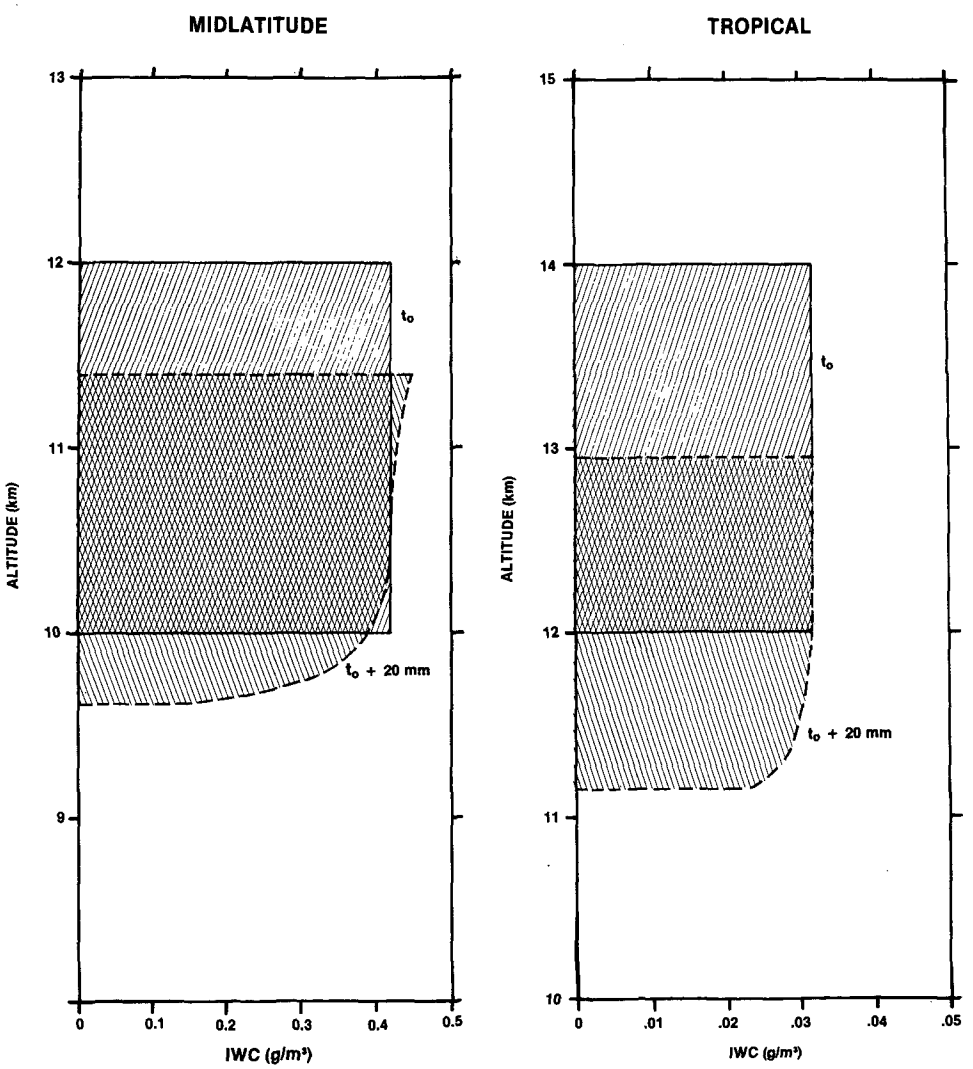

FIG. 2. Cloud ice water content profiles initially and after 20 min in the (a) midlatitude; and (b) tropical simulations.

Despite the simplicity of the model, these simulated lifetimes are within the range of observed lifetimes for both contrails, and for large cirrus layers in the absence of strong atmospheric dynamics (e.g., the anvil cloud left after a thunderstorm collapses). This suggests that cloud lifetime is basically determined in these circumstances by the time it takes to mix cloudy air with surrounding dry air. The details of the mixing may be of secondary importance. In the case of the present model "mixing" is achieved by letting the ice particles simply sediment into dry air, while in "reality" mixing may also include turbulent entrainment of dry air into a (growing) cloud volume. In some circumstances, sedimentation may be the rate-determining process.

a. Effects of latent heating

Vertical profiles of radiative and latent heating for each case are shown in Fig. 3. Latent heating is slight but most evident at the lower cloud boundaries at the beginning of the simulations. The radiative term is significant throughout the depth of these moderately thick clouds and dominates the latent term in both cases. The particles at cloud base evaporate more rapidly in the lower altitude, warmer midlatitude cloud.

The net radiative cooling shown at cloud top is the sum of solar heating and longwave cooling with the solar heating having an absolute magnitude equal to 44% that of the longwave cooling in the tropical case, and 36% in the midlatitude case. Solar heating decreases downward through the layer and is negligible at cloud base relative to longwave heating.

These profiles show that latent heating can contribute a significant portion to particle energy budgets only when conditions are significantly different from saturation (as they are at cloud base), as was discussed in more detail in Ramaswamy and Detwiler (1986). Cal-

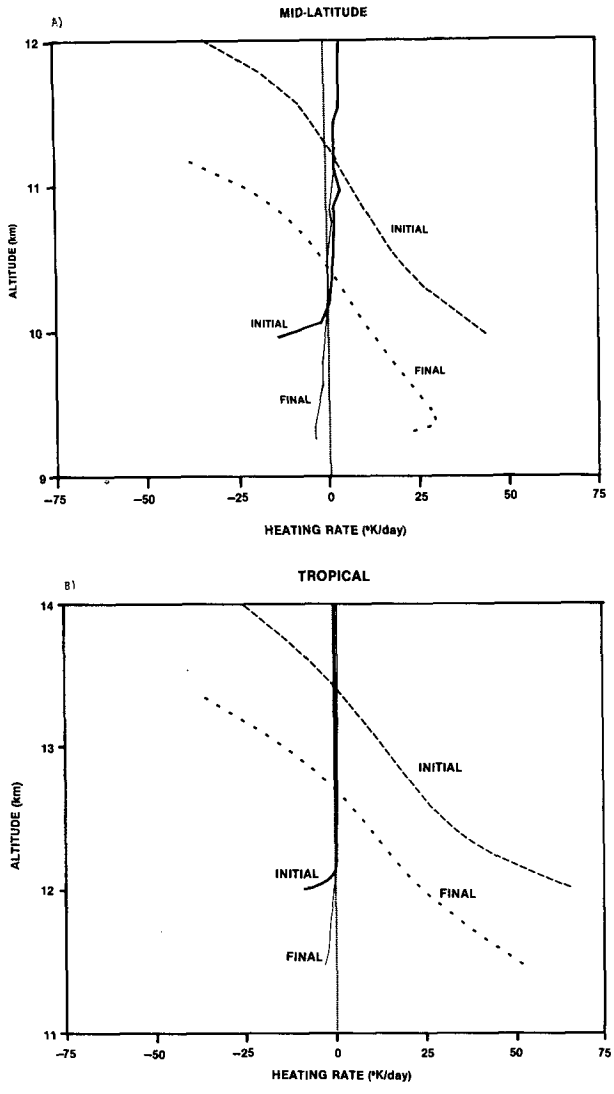

FIG. 3. Solid lines show heating profiles due to phase changes and dashed lines show radiative heating profiles, at the beginning and end of the simulations in (a) midlatitude; and (b) tropical atmosphere. The heavier lines represent the initial profiles; the lighter lines, the final profiles.

culations of the rate at which a cloud layer may become convectively unstable due to differential radiative heating will overestimate this rate if radiative heating at cloud base is presumed to be total heating in both of the situations shown in Fig. 3.

b. *Effects of cloud settling*

The integrated effect of the heating of the interstitial air due to the particles passing through is shown in Figs. 4a and 4b for the two cases. Only radiative and latent heat exchanges can affect air temperature in the model. The lighter curves show net changes in air temperature in the layers through which the cloud settles over a 20-min period. Also shown is a heavier curve representing the instantaneous net heating profile at the midpoint of the time interval.

The purpose of Fig. 4 is to show the difference in profiles of net heating that would be estimated if one computed net changes at a given time and assumed them to be representative of the heating rates for a 20-min period centered on that time, compared to the case where one integrates in small time-steps over the entire period.

The midlatitude case in Fig. 4a shows strong instantaneous cooling at cloud top and strong heating at cloud base of roughly equal magnitude at the midpoint of the 20-min simulation. As the cloud settles, the upper cloud layers can be expected to cool the air that has just been warmed by the passage of the lower cloud. The air that initially corresponds to cloud top is cooled at a high rate but experiences this cooling for only a short time so that the integrated amount of cooling at the altitude of the cloud top is smaller than might be inferred from the "instantaneous" curve. The net heating/cooling rate couplet, integrated over 20 min, has about the same gradient as the instantaneous one, but is limited to the middle two-thirds of the layer rather than the total layer depth, as might be inferred from the instantaneous profile at the midpoint of the time interval.

Similar patterns appear in Fig. 4b, describing results for the tropical case. In both cases, a given air layer is first heated as cloud base falls through it. As the cloud falls farther there is a transition to decreased heating of this layer and then cooling as the cloud top falls through it. A given volume of air does not experience just heating or just cooling for a prolonged period of time for clouds described by the parameters given in Table 1.

To further illustrate the differences between the computed vertical heating profile at a given instant, and the integrated heating profile observed over a length of time, one model run was extended to 60 minutes. The situation simulated was similar to the tropical cloud described in Table 1, but with particle size increased to 250 μm and concentration reduced to 32/l to yield a solar optical thickness of 0.49. The use of larger particles accentuates the effect of cloud settling and stretches out the heating profile in the vertical. The lower optical depth results in a cloud that is initially heated almost throughout its depth by planetary radiation from below. Results are shown in Fig. 5. Instantaneous total heating rate profiles are shown at the beginning and end of the simulation in Fig. 5. Latent heating and radiative heating, again, are the only two components in "total" heating. The net air temperature change over the one-hour period is also displayed. Note that the cloud is 2 km thick at the beginning and 1.3 km thick at the end of the hour, and that cloud top falls 3 km during the hour.

Heating rate profiles at any instant during the hour would suggest a differential heating rate of $\sim$1.1°K

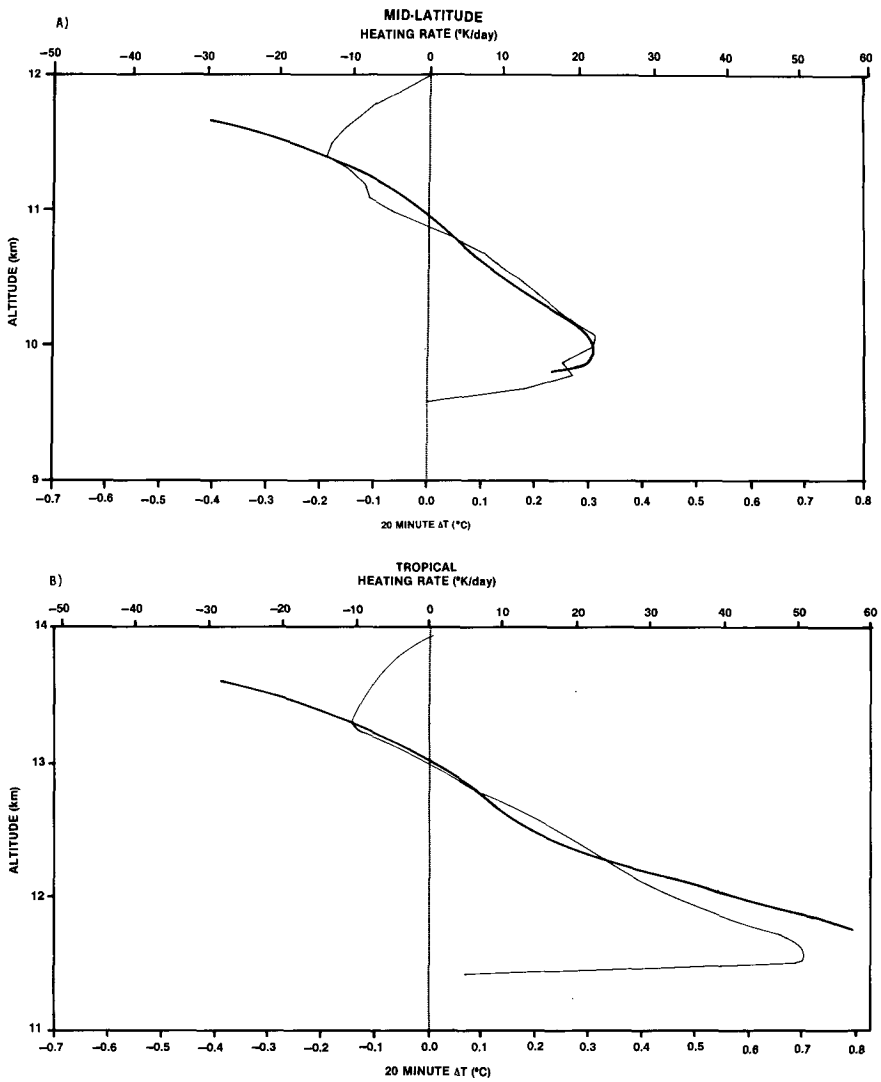

FIG. 4. Heavy lines show instantaneous total heating rates at the midpoint time, while light lines show integrated heating of the air through which the cloud falls during 20-min simulations in (a) midlatitude; and (b) tropical cases.

h^{-1} spread over an altitude difference of $\leqslant 2$ km. Note that the heating/cooling values at cloud top and base that contribute to the differential are quite different at the beginning and the end of the simulation. At the beginning there is heating through most of the cloud, strongest at the base, while at the end there is cooling in the upper half and heating in the lower half. As the cloud settles, the top particles begin to catch up to the smaller evaporating particles at the base. Due to this contraction, the rate of radiative destabilization might even be expected to increase as the layer compresses. However, the integrated heating rate curve suggests a much smaller overall differential heating rate of $\sim 0.6°K\ h^{-1}$ spread over 4 km. Between 11 and 12 km (just above the final cloud top) is the strongest gradient in net heating, $\sim 0.5°K\ h^{-1}$ difference over 1 km.

The integrated heating profile is complicated by the fact that as the cloud falls into lower warmer air layers there is an increasing tendency for stronger cloud top cooling and weaker cloud base heating. Optical depth also decreases from 0.49 to 0.46 over the 1-h simulation due to evaporation at cloud base. As the cloud falls there is an increasing tendency for cloud top cooling to cancel out the heating first produced by the cloud base particles as the cloud falls through an air layer. Latent heating plays an insignificant role in this case.

The simplicity of the model precludes precise comparison to all but the simplest "real" clouds. There is, however, a strong suggestion in Figs. 4 and 5 that rates of radiative destabilization may be overestimated if they are based on computed radiative heating rates in a cloud layer presumed to remain at a constant altitude

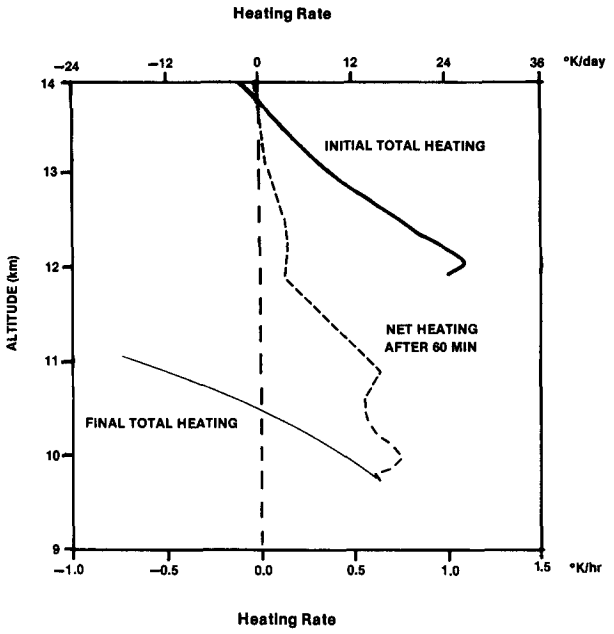

FIG. 5. Solid lines show initial and final total heating rate profiles, while the dashed line shows integrated air temperature change during a 60-min simulation in the tropical atmosphere.

in a fixed volume of air. Even the values of the in-cloud heating/cooling rate profile may be prone to inaccuracies in a nondynamic cloud computation.

It might seem more realistic to assume that the cloud layer is suspended in upward moving air so that it does not fall towards the ground. In such a situation, though, the rising air must pass through the cloud. The stretching of the net air heating profile must occur in a manner somewhat similar to that shown in Fig. 5, only in a frame of reference fixed to the upward moving air.

c. *Variations with cloud altitude and microphysical properties*

A limited exploration was made of the parameter space of this simple cloud model in order to place the above results for two-kilometer thick clouds in perspective. The effects of particle concentration and particle size (optical thickness), saturation ratio (SR), cloud altitude, and diurnal variations on heating rates are shown in Table 2. These are instantaneous values corresponding to conditions at the altitudes indicated in the corresponding standard atmosphere with cloud properties as in Table 1, except as otherwise indicated.

Figure 6 shows radiative and phase-change (latent) heating for the same cloud at three different altitudes in both tropical and midlatitude situations. The middle altitude in each situation corresponds to the "standard" case described in Table 1. A numerical summary can be found among the results given in Table 2. The comparison is somewhat artificial because in the actual troposphere cloud microphysical properties vary predictably with altitude, with a trend towards smaller particles and lower ice contents at higher altitudes (Heymsfield and Platt 1984).

In the tropical case, the tendency for radiative heating at cloud base increases with altitude as the base temperature decreases, while the tendency for cooling at cloud top decreases with altitude as the top temperature decreases. This is to be expected, as the cloud top temperature approaches that of the effective sky temperature and the cloud base becomes colder relative to the effective ground temperature as cloud altitude increases. Others (Ackerman et al. 1988) have noted similar tendencies in tropical cirrus cloud simulations. In the midlatitude case, both cloud top cooling and cloud base heating increase with altitude. Unlike the tropical case, the effective sky temperature is still de-

TABLE 2. A summary of cloud top and cloud base radiative heating/cooling, and ratio of latent-to-radiative effects, for cirrus cloud cases examined in this study.

	Energy budget summaries				
	Top		Base		
Case	Radiative	Latent / radiative	Radiative	Latent / radiative	Solar optical depth
Midlatitude, stnd.	−28.6	−0.12	+40.1	−0.37	.75
Midlatitude, wet	−28.6	−0.64	+40.1	−0.16	.75
Midlatitude, dry	−28.6	+0.54	+40.1	−1.10	.75
Tropical, stnd.	−26.6	−0.03	+66.6	−0.14	.75
Tropical, wet	−26.6	−0.22	+66.6	−0.07	.75
Tropical, dry	−26.6	+0.19	+66.6	−0.38	.75
Tropical, small size	+6.62	+0.01	+5.05	−0.11	.17
Tropical, low conc	+7.1	+0.00	+8.2	−0.21	.22
Tropical, high conc	−119.5	−0.01	+251.8	−0.12	1.85
Tropical, large size	−82.1	−0.02	+312.5	−0.22	2.31
Tropical, night	−48.3	−0.02	+65.5	−0.14	.75

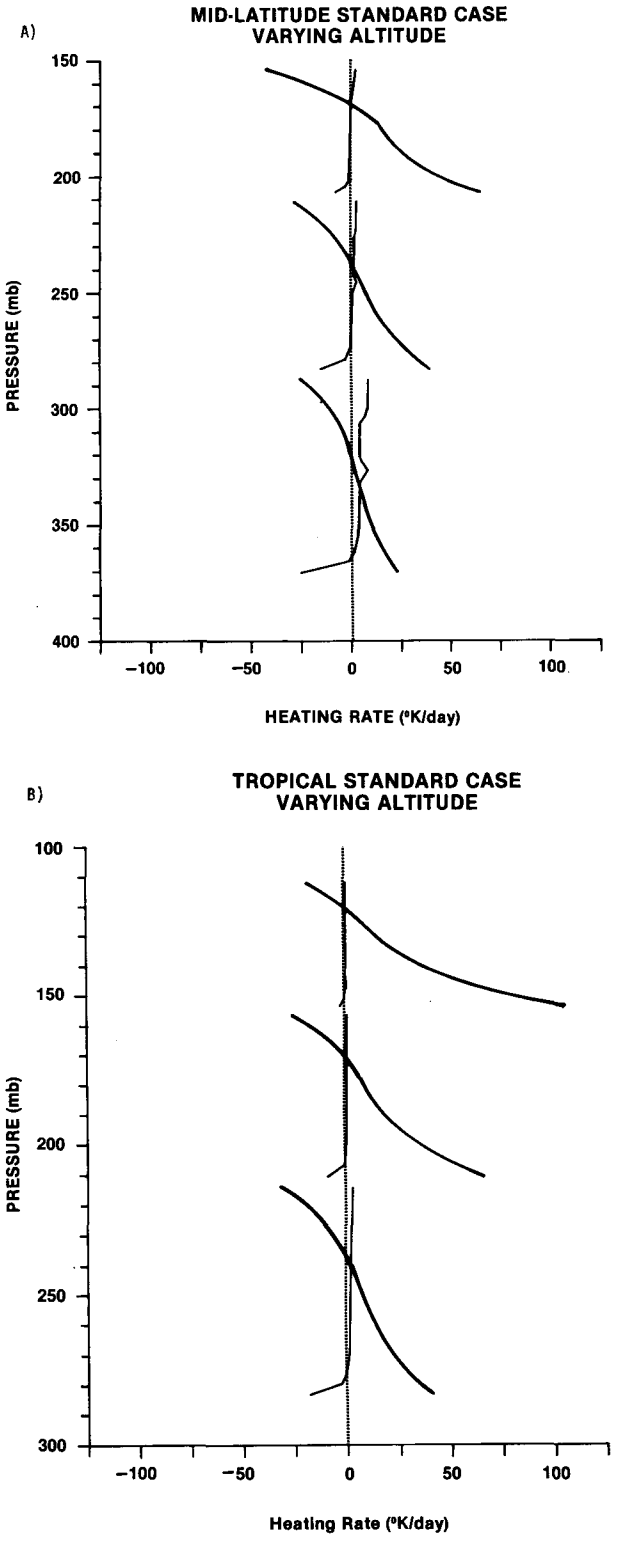

FIG. 6. Vertical profiles of the instantaneous latent (light lines) and radiative (heavy lines) heating inside cloud with top and base at various altitudes in (a) midlatitude; and (b) tropical standard atmospheres. For each atmosphere, the results for the middle cloud represent the standard case defined in Table 1, and also shown in Fig. 3.

creasing with altitude over the altitude range explored in the midlatitude case.

The difference in heating rates between base and top increases with altitude for these moderately thick clouds in both atmospheres.

At the lowest altitudes shown in each atmosphere, sublimational cooling at cloud base is nearly equal to radiative heating. The magnitude of cloud base sublimational cooling decreases with altitude and becomes negligible at the highest altitude studied in each atmosphere. Cloud base saturation ratio is 0.85 in all cases, but the rate of sublimation decreases as cloud base temperature decreases. This is due to the decrease in the vapor density gradient corresponding to a given saturation ratio gradient (i.e., the lower saturation vapor density over ice at lower temperatures). As the rate of sublimation decreases, so must the sublimational (latent) cooling.

The influence of variations in saturation ratio at cloud base and cloud top for the otherwise standard conditions was tested. A "wet" case was simulated with SR set to 1.15 at the initial altitudes of the top three 100 m thick layers and SR = 0.95 below initial cloud base. A "dry" case was simulated with SR = 0.85 at the initial altitudes of the top three layers and SR = 0.5 below initial cloud base. Results are found among the cases displayed in Table 2. Latent heat effects are stronger at cloud top in the "wet" cases due to strong particle growth, and at cloud base in the "dry" cases due to stronger sublimation. The cloud base SR in the "dry" case is 0.5, which is not an extreme value at cirrus altitudes. For nearly saturated conditions at cloud base, loss of latent heat due to evaporation is small compared to radiative heating in both tropical and midlatitude atmospheres. Latent heating is generally of less relative importance in the colder tropical environment.

Figure 7 shows the effect of increasing particle concentration for a given particle size at the standard altitude in the tropical atmosphere. Numerical results for this case are also contained in Table 2. As particle concentration increases, so does optical thickness; and the differential heating rate across the cloud becomes larger. The relative magnitude of latent heating compared to radiative heating is important only at cloud base. Figure 7 shows that there is weak net heating throughout the cloud for low concentrations (small optical thickness) and strong differential heating for large concentrations (large optical thickness), similar to results reported by others (Ackerman et al. 1988).

Variation of particle size with a fixed concentration results in changes in optical thickness and changes in heating rate profiles similar in character to those shown in Fig. 7. Numerical results for this case can be found in Table 2. For the case of the smallest particles (50 μm), the fallspeed is reduced to ~30% of the standard 150 μm particle, so the stretching of the integrated net heating profiles compared to the instantaneous ones

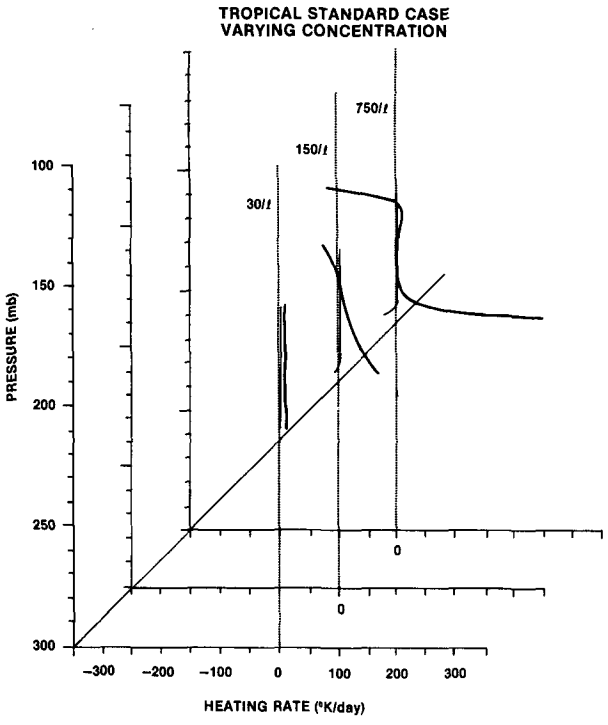

FIG. 7. Vertical profiles of the instantaneous latent (light lines) and radioactive (heavy lines) heating inside three clouds with three different particle concentrations at the altitude of the standard case in a tropical atmosphere. The concentrations are 30/l, 150/l ("standard" tropical case), and 750/l.

shown in Figs. 4 and 5 is correspondingly reduced (not shown). For the largest particle (500 μm), the fallspeed is ~3 times larger compared to a 150 μm particle, and the stretching is correspondingly accentuated (also not shown).

The effect of diurnal variations was also investigated by eliminating solar flux from the tropical standard case. Results can be found in Table 2. For this moderately thick cloud, solar heating is not strong near cloud base, but is significant at cloud top having an absolute magnitude of ~50% of the infrared cooling. This suggests that radiative destabilization of moderately optically thick clouds might occur more readily at night. Starr (1987) has examined diurnal variations in optically thinner cirrus clouds with his two-dimensional dynamic cloud model, including bulk microphysics and radiative interactions. His results suggest that radiative coupling with dynamics is quite complex and that it may not be possible to make strong inferences from simple nondynamical models.

There are other parameters to which model results are sensitive. Surface albedo was fixed at 0.1 for all simulations. Higher surface albedo, such as that produced by land or lower cloud layers, would have increased the relative impact of solar heating. Surface temperature affects incident infrared flux at cloud base, but was fixed at 294°K in the midlatitude atmosphere and 300 K in the tropical atmosphere. There are a large number of sensitivity studies that could be presented. The results given here are restricted to those important to the main thrust of the investigation at hand, which is to try to understand the effects of latent heating and particle sedimentation on the vertical profile of net air heating as cirrus clouds evolve in still air.

One of the strong simplifications used in this work is the assumption of monodisperse particle sizes within a 100 m thick layer. In this Lagrangian model, monodisperse sizes mean that there is a unique fall velocity associated with each layer resulting in great computational simplicity. The same simplification is implicitly made in bulk microphysical Eulerian models, such as that of Starr and Cox (1985a). In the simplest of such models a single velocity, a single characteristic optical cross section, etc., is assigned to cloud mass at a given grid point. In the context of the model used here, polydisperse particle sizes would lead to a further stretching of the cloud in the vertical with time: small particles falling slower, large ones faster. The effects on net heating curves would no doubt be quite complex because fallspeeds, particle growth/evaporation, and radiative absorption are highly dependent on the particle surface area distribution, non-sphericity, etc., in addition to the parameters discussed above. An extension to allow a distribution of particle sizes; as well as changes in that distribution due to nucleation, aggregation, and breakup; is perhaps the most useful enhancement that can be made to the model in its current state.

4. Conclusions

A computational study has been made of the relative importance of particle fallspeed and vapor deposition/sublimation in the net thermal energy exchange between cirrus cloud particles and the atmosphere through which they are falling. Two-kilometer thick cloud layers were inserted in tropical and midlatitude atmospheres and their evolution followed long enough to show the following tendencies:

1) Latent heat exchange tends to oppose the sense of radiative heating. Particle sublimation at cloud base and growth at cloud top partially counteract the tendency for clouds to heat radiatively at their bases and cool at their tops, respectively. For the 2-km thick cloud layers considered, latent heating is a significant fraction of radiative heating at cloud base near and below tropopause heights in the situations simulated. Latent heating at cloud base becomes insignificant above 12 km in the midlatitude atmosphere and above 14 km in the tropical atmosphere. It is generally insignificant at cloud top relative to radiative cooling. Latent heating is more significant, and can dominate radiative heating, for saturation ratios further from unity, as might be expected.

2) The settling of the cloud layer tends to stretch its heating effects in the vertical. As a layer of cloud par-

ticles settles through the air, infrared heating at cloud base first heats the air. Later, the rest of the cloud falls through this same air. Infrared cooling near cloud top cools the air that had been previously heated. The net effect is sensitive to the altitude, radiative environment, and cloud microphysical properties.

The results presented here are highly idealized. If one were to identify them with an actual situation in the "real" atmosphere, they would most closely describe the evolution of the peripheral regions of thunderstorm anvils. It is clear in these situations that neglecting particle volatility and the movement of cloud particles relative to the air may result in an overestimate of the rate at which such clouds might become radiatively destabilized. There may also be misrepresentation of the time-integrated radiative heating/cooling values at cloud top and base if the movement of the cloud in the vertical is ignored.

This study, and those discussed in the introduction, all make partial representations of real cirrus cloud phenomena, treating some aspects in great detail and others more crudely. Although the physics of these clouds can, in principle, be represented with a fairly high level of complexity (given enough computing power), there is still a dearth of in situ observational evidence concerning actual cloud physical properties and the dynamic, thermodynamic, and radiative properties of cirrus cloud environments. A better mapping of the range of typical boundary conditions is required to enable models to be used to better diagnose the factors most strongly influencing cirrus cloud evolution in the atmosphere.

Acknowledgments. This study was conducted with partial support from the National Science Foundation under Cooperative Agreement ATM-8620145 and the State of South Dakota. Helpful comments by Drs. S. Manabe and J. D. Mahlman are acknowledged.

REFERENCES

Ackerman, T. P., K.-N. Liou, F. P. J. Valero and L. Pfister, 1988: Heating rates in tropical anvils. *J. Atmos. Sci.*, **45,** 1606–1623.

Bennetts, D. A., and M. Ouldridge, 1984: An observational study of the anvil of a winter maritime cumulonimbus cloud. *Quart. J. Roy. Meteor. Soc.*, **110,** 85–103.

Danielsen, E. F., 1982a: A dehydration mechanism for the stratosphere. *Geophys. Res. Lett.*, **9,** 605–608.

——, 1982b: Statistics of cold cumulonimbus anvils based on enhanced infrared photographs. *Geophys. Res. Lett.*, **9,** 601–604.

Detwiler, A. G., and R. W. Pratt, 1984: Clear-air seeding: Opportunities and strategies. *J. Wea. Mod.*, **16,** 46–60.

Foot, J. S., 1988: Some observations of the optical properties of clouds. II: Cirrus. *Quart. J. Roy. Meteor. Soc.*, **114,** 145–164.

Griffith, K. T., S. K. Cox and R. Knollenberg, 1980: Infrared radiative properties of tropical cirrus clouds inferred from aircraft measurements. *J. Atmos. Sci.*, **37,** 1077–1087.

Hall, W. D., and H. R. Pruppacher, 1976: The survival of ice particles falling from cirrus clouds in subsaturated air. *J. Atmos. Sci.*, **33,** 1995–2006.

Heymsfield, A. J., 1972: Ice crystal terminal velocities. *J. Atmos. Sci.*, **29,** 1348–1357.

——, 1975: Cirrus uncinus generating cells and the evolution of cirriform clouds. Part I. Aircraft observations of the growth of the ice phase. *J. Atmos. Sci.*, **32,** 799–808.

——, 1986: Ice particle evolution in the anvil of a severe thunderstorm during CCOPE. *J. Atmos. Sci.*, **43,** 2463–2478.

——, and C. M. R. Platt, 1984: A parameterization of the particle size spectrum of ice clouds in terms of the ambient temperature and ice water content. *J. Atmos. Sci.*, **41,** 846–855.

Knollenberg, R. G., A. J. Dascher and D. Huffman, 1982: Measurements of the aerosol and ice crystal populations in tropical stratospheric cumulonimbus anvils. *Geophys. Res. Lett.*, **9,** 613–616.

Lilly, D. K., 1988: Cirrus outflow dynamics. *J. Atmos. Sci.*, **45,** 1594–1605.

Paltridge, G. W., and C. M. R. Platt, 1981: Aircraft measurements of solar and infrared radiation and the microphysics of cirrus clouds. *Quart. J. Roy. Meteor. Soc.*, **107,** 367–380.

Ramaswamy, V., 1988: Dehydration mechanism in the Antarctic stratosphere during winter. *Geophys. Res. Lett.*, **15,** 863–866.

——, and J. T. Kiehl, 1985: Sensitivities of the radiative forcing due to large loadings of smoke and dust aerosols. *J. Geophys. Res.*, **90,** 5597–5613.

——, and A. Detwiler, 1986: Interdependence of microphysics and radiation in cirrus clouds. *J. Atmos. Sci.*, **43,** 2289–2301.

Sassen, K., D. O'C. Starr and T. Uttal, 1989: Mesoscale and microscale structure of cirrus clouds: Three case studies. *J. Atmos. Sci.*, **46,** 371–396.

Starr, D. O'C., 1987: Effects of radiative processes in thin cirrus. *J. Geophys. Res.*, **92,** 3973–3978.

——, and S. K. Cox, 1985a: Cirrus clouds. Part I: A cirrus cloud model. *J. Atmos. Sci.*, **42,** 2663–2681.

——, and ——, 1985b: Cirrus clouds. Part II: Numerical experiments on the formation and maintenance of cirrus. *J. Atmos. Sci.*, **43,** 2695–2698.

Stephens, G. L., 1983: The influence of radiative transfer on the mass and heat budgets of ice crystals falling in the atmosphere. *J. Atmos. Sci.*, **40,** 1729–1739.

Warren, S. G., 1984: Optical constants of ice from the ultraviolet to the microwave. *Appl. Opt.*, **19,** 3057–3067.

Welch, R. M., S. K. Cox and J. M. Davis, 1980: Radiation and clouds. *Meteor. Monogr. No. 39,* Amer. Meteor. Soc., 96 pp.

Wendling, P., 1980: On the interaction of radiation and cirrus clouds in the infrared window region. *J. Rech. Atmos.*, **14,** 399–407.

Wiscombe, W. J., 1977: The delta-Eddington approximation for a vertically inhomogeneous atmosphere. NCAR Tech. Note NCAR/TN-121&STR, 66 pp.